# High Power (>1W) Application RF MEMS Lifetime Performance Evaluation

*Joanne Wellman – Jet Propulsion Laboratory*
*Adalberto Garcia – California State University, Northridge*

## 1.0 *INTRODUCTION*

Solid-state RF devices are currently utilized in a wide array of application areas, including satellite communications systems, wireless communications systems, automotive radars, and defense applications. Currently, PIN diode or Field Effect Transistor (FET)-based switches are utilized for their high switching speeds, high power handling, low drive voltage, low cost, and technology maturity – reliability and performance assurance characteristics can be drawn from the extensive history of semiconductor reliability research.

MEMS RF technologies offer the advantages of low power consumption (near zero), low insertion loss (~0.1dB up to 40 GHz), and high isolation (>40dB), as well as low volume and low mass. Because of these advantages, RF MEMS has been identified as one of the target technologies that could see high production in the next several years and capture an increased market share[1]. The commercial sector has recognized the potential for large-scale RF MEMS switch production, primarily for telecommunications applications, and the race is on for developing a robust integrated RF MEMS switch design. The DARPA MEMS program is also supporting RF MEMS switch development for defense, space, and satellite applications[2].

The imminent introduction of RF MEMS to the COTS market makes the following questions of immediate relevance: What are the performance limitations for RF MEMS devices? What are the reliability implications for incorporating RF MEMS devices into a space flight board assembly? This is not easily answered for several reasons. First, MEMS, as a technology, is still in its infancy and there is much work in the area of MEMS reliability that has not yet been done. Second, there is no standard RF MEMS design (e.g. RF MEMS switch) and the failure modes for MEMS are highly design-dependant. Third, most of the RF MEMS device reliability research performed in the commercial sector is proprietary, unpublished and unavailable. In this study, we evaluate the performance of an RF MEMS device under the conditions for spacecraft communications transmission (>1W) in an effort to evaluate RF MEMS switch technology for space flight readiness.

## 2.0 *MOTIVATION*

The performance advantages outlined above make the infusion of RF MEMS switches (and filters) into NASA spacecraft an exciting leap toward faster, more powerful communications and radiometric systems. For example, currently available commercial RF transceiver solutions are nearing fully integrated on-chip systems, but the switches (and resonators) remain off-chip components. MEMS switches (and MEMS resonators) can help the industry reach fully integrated communications subsystems. In the case of the transceiver, lower insertion loss in the switches between the antenna and the first low-noise amplifier (LNA) leads to lower noise figures and higher sensitivity of the receiver. This effect is magnified when more than one antenna is used, which requires additional switches in the antenna-LNA path. Half duplex systems utilize RF switches to switch between transmit and receive modes. Redundant systems use RF switches to change between redundant segments. Multiple antenna systems, such as diversity receivers or ping-pong mode radar systems, use RF switches for antenna switching. Virtually all spacecraft with communications or radiometric systems employ such configurations

and their performance currently suffers from high insertion loss/low isolation in solid-state RF switches.

This work was performed in support of the MEMS PICOSAT Inspector (MEPSI) program funded by DARPA/AFRL. JPL led the project with the Aerospace Corporation as the primary sub-contractor. The first flight in the MEPSI program is on the Space Shuttle (STS-113) and has as its mission objectives, the demonstration of several MEMS devices including the MEMS transmit-receive (TxRx). The 1-kg class satellite plans to use the MEMS TxRx switch as a functional component on its RF communication board. This study was designed to simulate the mission requirements of ~1W transmitted RF power at 915MHz for a 2 week mission lifetime, beaconing 1/sec for a total of at least 1.2 million cycles.

Most lifetime testing of RF MEMS devices, up to 500 million cycles, has been carried out at input RF powers of a few mW's[3]. The primary cause of failure in contact MEMS switches is degradation of the contact area metal due to repeated impact between the base and the suspended beam. Pitting, wear, metal migration, and contamination can all contribute to a significant increase in contact resistance and insertion loss. The failure rate is amplified when operating at RF powers over 100mW because microwelding can bond the pads together, resulting in a permanent short failure[3]. Verification of successful increased power handling broadens the potential application of RF switches in communications systems and makes this work especially relevant for RF MEMS space flight performance assurance.

## 3.0 *DEVICE DESCRIPTION*

The devices of this study were metal-contact switches under ongoing development by the Rockwell Scientific Corporation (RSC). The RSC MEMS switch is a suspended bridge-type mechanical relay fabricated on GaAs substrate, with PECVD dielectric mechanical structures and Au-based contact metallization. Design and fabrication details are described elsewhere[4]. The TxRx devices used in this study were single pole double throw switch devices made up of a configuration of 3 RF MEMS switches (see Figure 1), one RF MEMS switch in the receive (Rx) line and two parallel relays in the transmit (Tx) line to accommodate the higher transmitted power. The relays were activated electrostatically by applying a dc control bias (see Table 1). These TxRx devices were designed, fabricated and packaged by RSC for inclusion in the MEPSI communications board.

| Applied Control Voltage (VDC) | RF MEMS Switch State |
|---|---|
| 70V/80V | Closed |
| 0V | Open |

**Table 1. Truth table for electrostatically actuated RSC RF MEMS switch.**

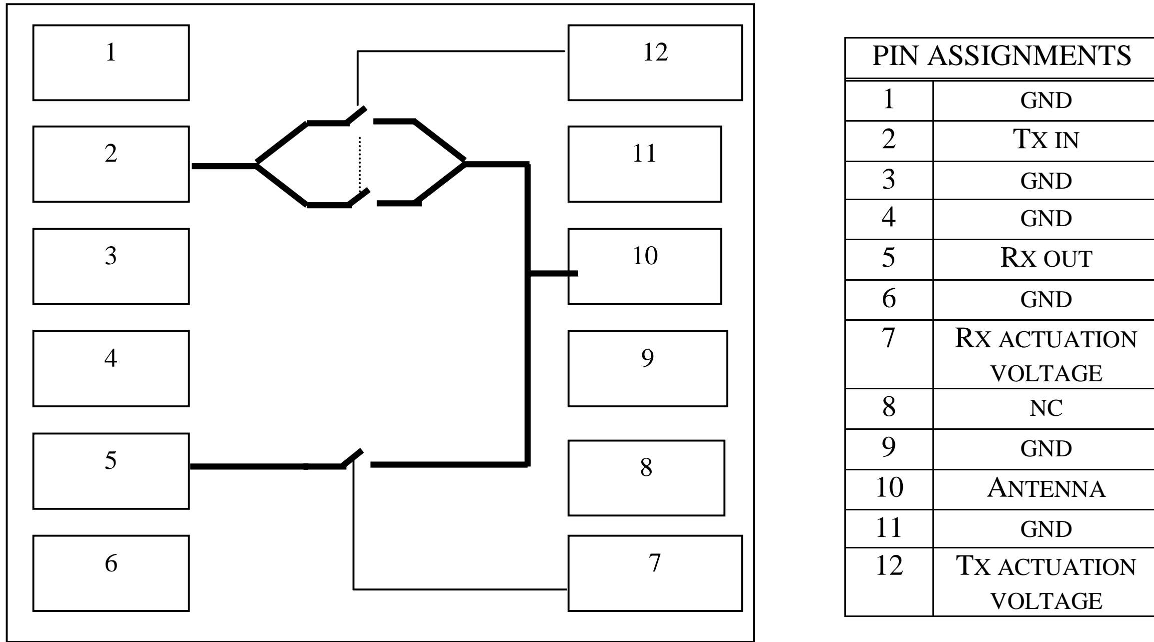

| PIN ASSIGNMENTS | |
|---|---|
| 1 | GND |
| 2 | TX IN |
| 3 | GND |
| 4 | GND |
| 5 | RX OUT |
| 6 | GND |
| 7 | RX ACTUATION VOLTAGE |
| 8 | NC |
| 9 | GND |
| 10 | ANTENNA |
| 11 | GND |
| 12 | TX ACTUATION VOLTAGE |

**Figure 1. Schematic and pinout of RSC TxRx device. The GND connections are for RF grounds conductors and all conduction lines are designed for 50Ω impedance.**

## 4.0 *TEST SET-UP*

A schematic of the experimental setup is shown in Figure 2.

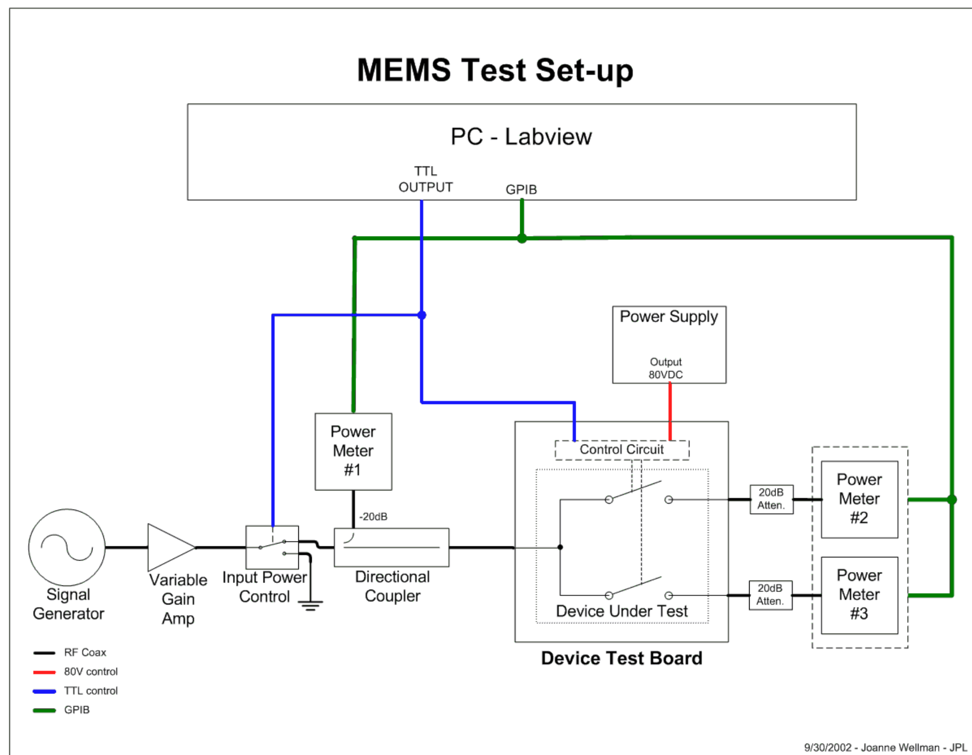


**Figure 2. Schematic of MEMS RF test set-up.**

An RF signal generator/variable gain amp supplied constant RF power to a TTL FET-based (Hittite HMC195) circuit (see Figure 3). The TTL signals were supplied by the computer I/O board and controlled the input power to the device under test. The circuit board used was of standard RF design, with 50-ohm signal lines and VIA holes connecting the top and bottom ground planes.

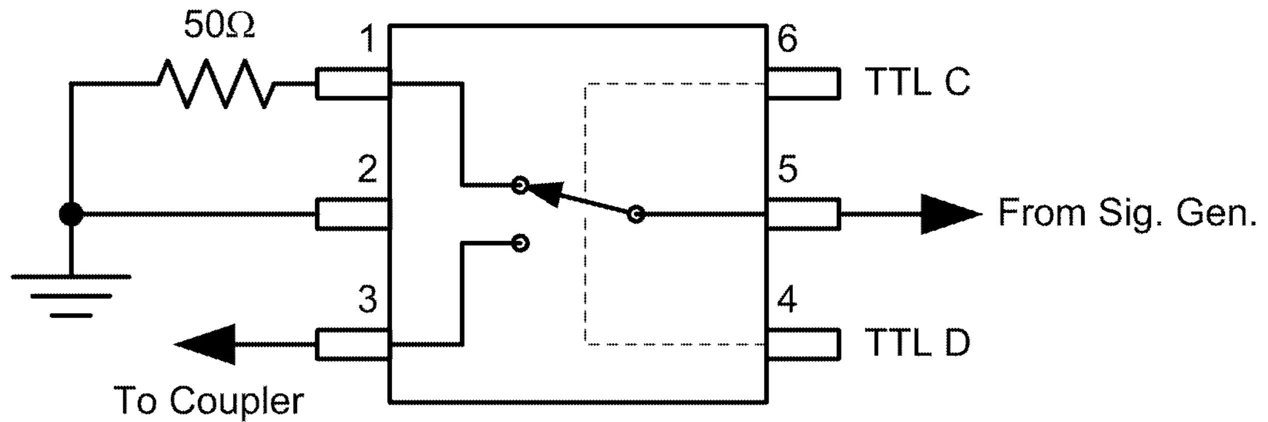


**Figure 3. Schematic of RF Input Power Control circuit.**

The packaged devices were mounted on a board designed for remote automated testing (see Figure 4). The test board was fabricated on a double-sided 63-mil FR4 board with a solid ground copper backplane and 50 ohm impedance signal lines. The 70V/80V actuation voltage supply to the RF MEMS switch was controlled by TTL-level signals from the computer I/O board.

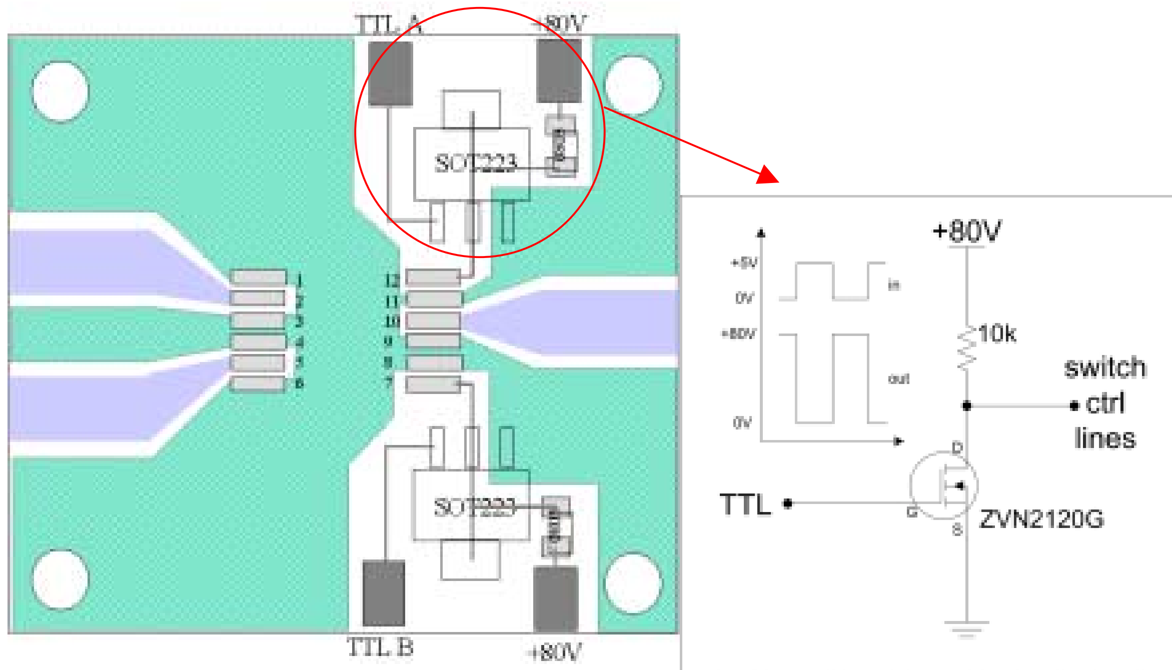


**Figure 4. Test board layout with detailed schematic of the actuation voltage supply control circuit.**

For this test, the input RF signal entered the TxRx device at pin 10 (ANT) and output powers were measured at pins 2 (Tx) and 5 (Rx), as well as at the sniffer port of the directional coupler (sampled input power). All power measurements were made on HP E4419B RF power meters with HP E4412A E series CW power sensor heads and were calibrated to account for cable/connector losses inherent in the test setup.

LabVIEW computer remote automation software controlled the relative timing of input RF signal, switch actuation voltage application, and data acquisition from the three power meters (see Appendix). A timing diagram is shown in Figure 6. Input power to the device was turned off as actuation voltages were changed, as hot switching introduces mechanisms that can result in permanent fail in the closed state (electrical short). A single test cycle was defined as measuring the power at ANT, Tx, and Rx in two configurations, Tx closed/Rx open and Tx open/Rx closed (see Figure 5). 1W of RF power at 915 MHz was applied to the device at each configuration for 100ms per cycle, as shown in Figure 6.

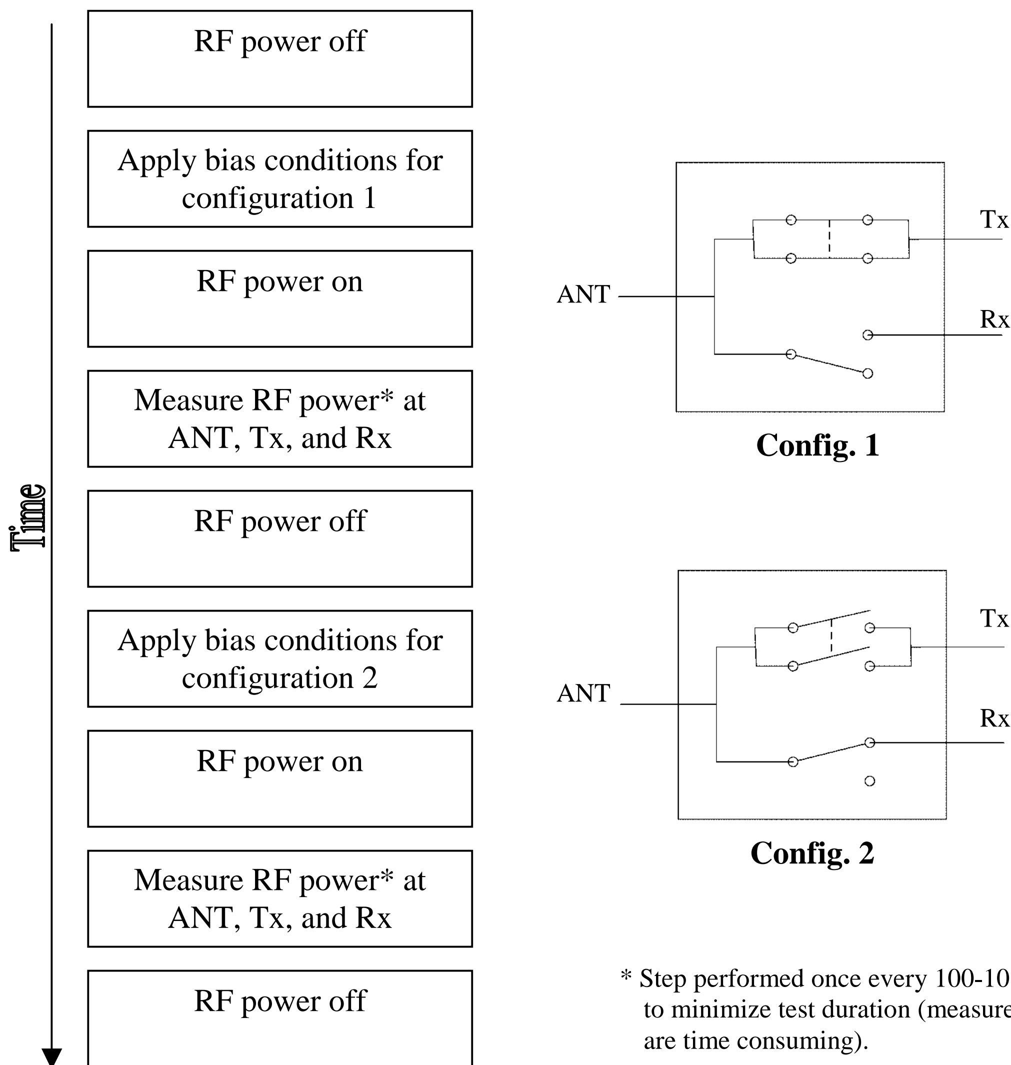


**Figure 5. Test flow diagram of a single cycle.**

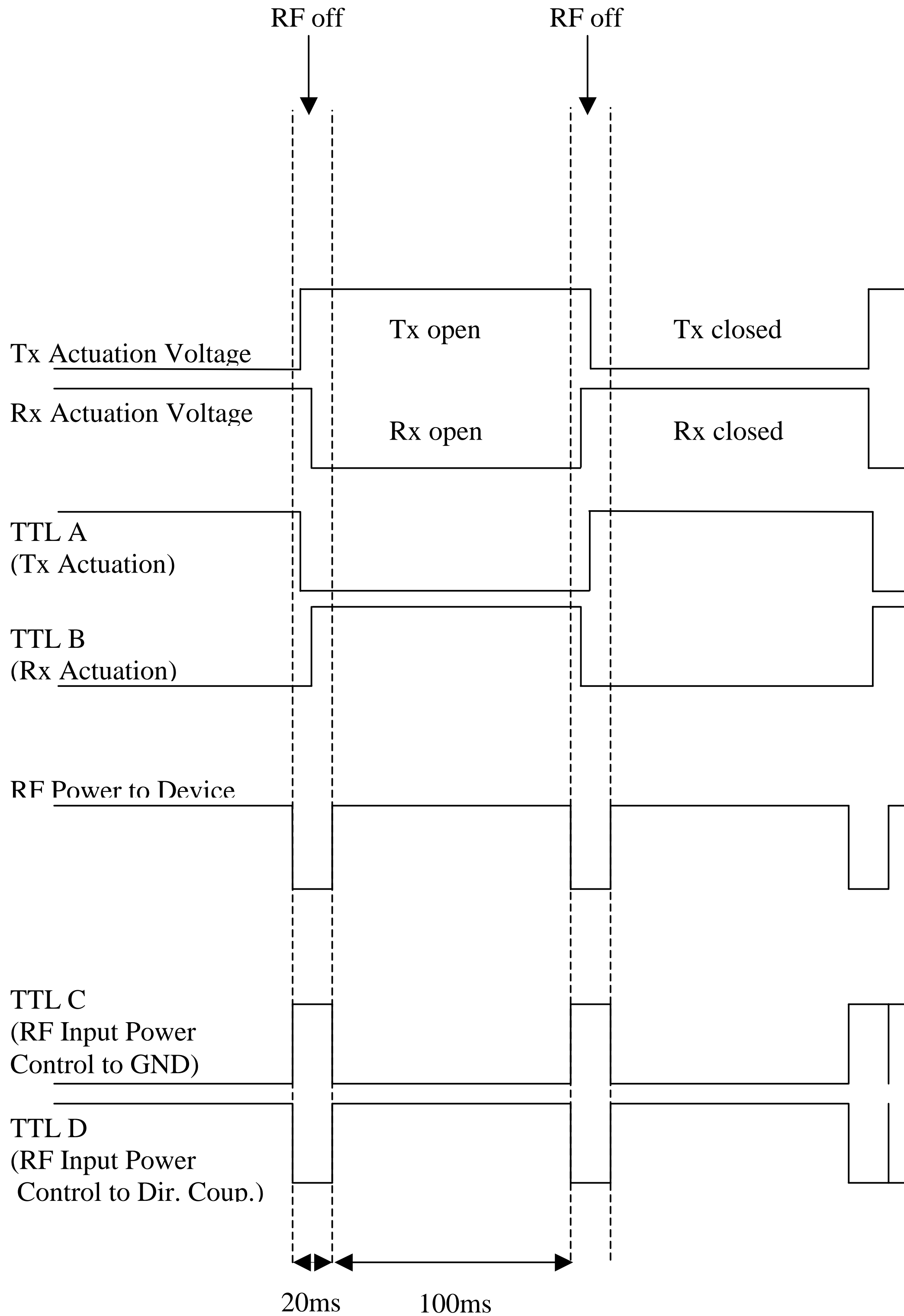


**Figure 6. Timing Diagram of switch cycling in LabVIEW control software**

## 5.0 *RESULTS*

Two TxRx devices were delivered by RSC for test, hereafter referred to as Device A (80V Control Bias design) and Device B (70V Control Bias design).

*Note:* The plots below illustrate measurements performed once every 100-10,000 switching cycles. RF input power was applied during each cycle for 100 ms.

### 5.1 Pre-test observations

*Device A:* Initial inspection revealed an intermittent short between pins 5 and 6 (Rx and GND). Because there were only two available test devices, Device A was included in the testing after ensuring that pin 6 was isolated from the board and that pin 5 was not shorted to ground at the beginning of the test and would thereafter be monitored. Post-test destructive inspection showed a broken bond wire to pin 6 that was in close proximity to, but not in contact with, wire bond 5.
*Device B:* Continuity checks with a multimeter showed no anomalous readings.

### 5.2 Data Acquisition

*Device A:* Device A was inserted into the test setup shown in Figure 2 as the Device Under Test. After initial performance checks at 0 dBm and 20 dBm (~100 cycles each), the RF power was increased to the full test value of 30 dBm (1W), calibrated at the device input pin. After 10 million cycles at 30 dBm, which exceeded the device performance requirement of 1.2 million cycles, the RF power was increased to 32 dBm to give 2 dB of margin over the proposed application. The device was then cycled until a failure occurred, defined as either a 20 dB increase in insertion loss of either path or a 20 dB decrease in isolation.
*Device B:* Failed in calibration portion of testing. Actuation voltage was toggled while RF power was applied. This single hot switch was enough to permanently fail the Rx line closed. No further cycling was performed.

### 5.3 Initial Observations

*Device A:* The Tx path failed open after approximately 17 million cycles, as shown in Figure 7 through Figure 10 below.
*Device B:* N/A

**Figure 7. ANT, Tx and Rx power meter measurements at ~1W RF input when switch is in Configuration 1 defined above (see Figure 5).**

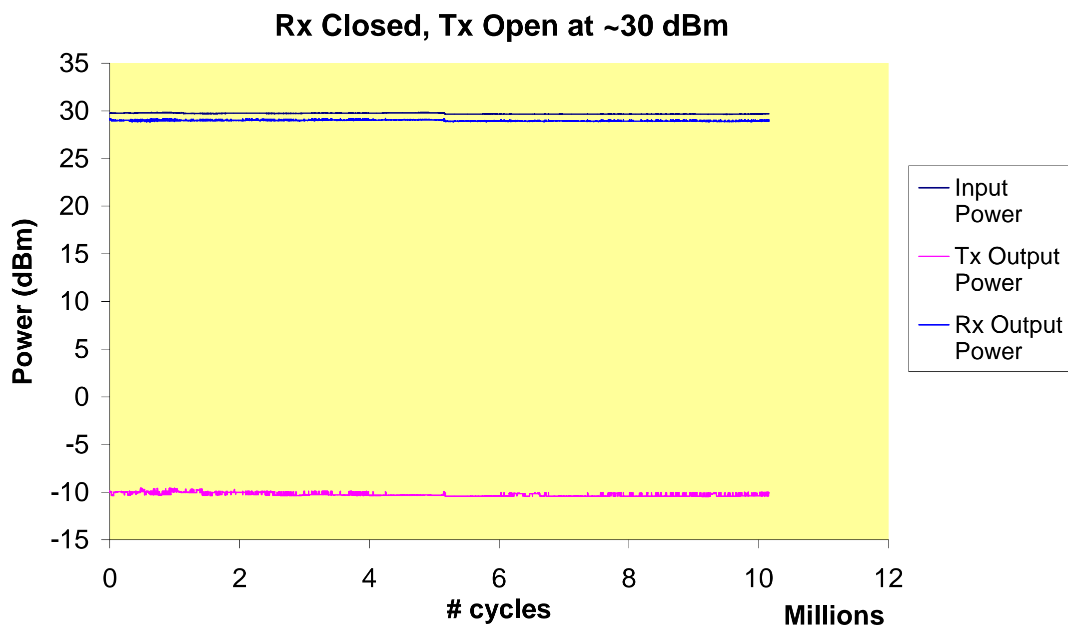


**Figure 8. ANT, Tx and Rx power meter measurements at ~1W RF input when switch is in Configuration 2 defined above (see Figure 5).**

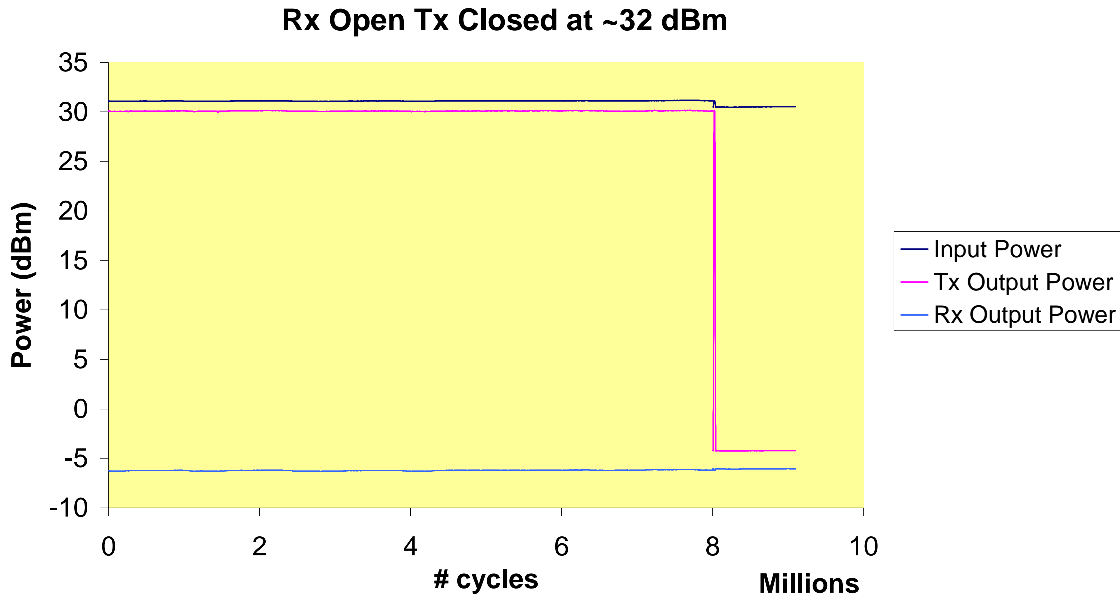


**Figure 9. ANT, Tx and Rx power meter measurements at ~1.5W RF input when switch is in Configuration 1 defined above (see Figure 5).**

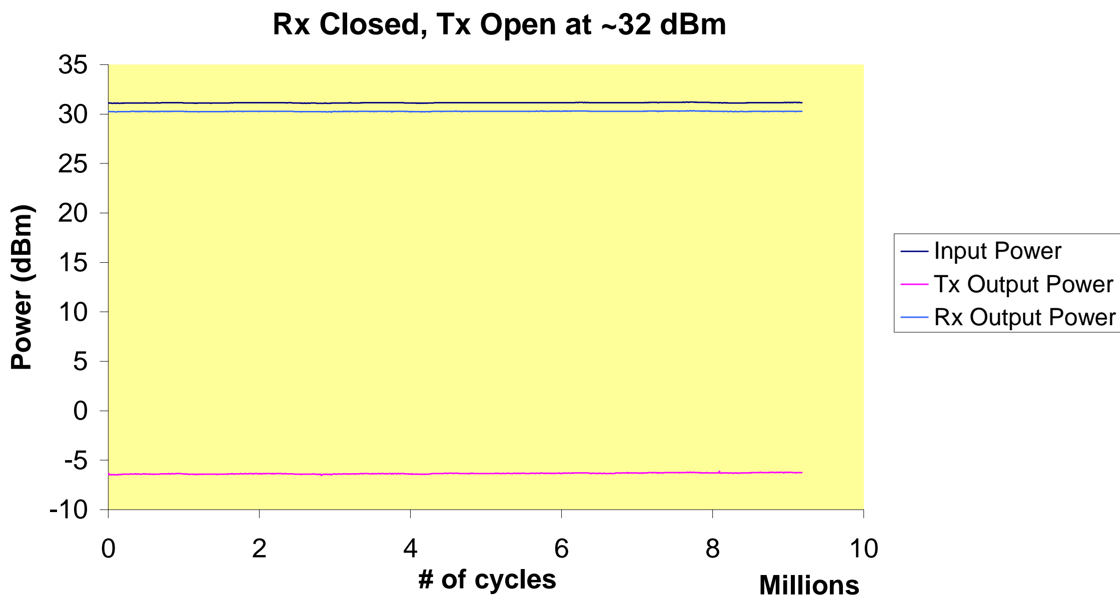


**Figure 10. ANT, Tx and Rx power meter measurements at ~1.5W RF input when switch is in Configuration 2 defined above (see Figure 5).**

## 6.0 *ANALYSIS*

With the limited number of samples provided it is impossible to completely characterize device functional ruggedness. Rather, the objective of this study was to assess the cycling lifetime reliability of selected devices. However, these results are relevant in assessing general performance capabilities of the technology and some conclusions can be drawn about these capabilities.

### 6.1 Failure Analysis

*Device A:* Device was imaged with SEM in the delidded package. Attempts to actuate the switch in the SEM resulted in the observation of a single closure of one switch in the Tx path. Further attempts to view dynamic switch operation were unsuccessful, perhaps due to interference of the electrons from the microscope's e-beam with the electrostatic actuation field. After the device was removed from SEM, the Tx path was no longer failed open and responded as expected to the 80V actuation voltage to the Tx pin. This is consistent with observations made by RSC that switch many-cycle failures were correlated with the presence of thin insulating layers between contacts and recovery is possible with procedures that remove some of the insulating material to restore electrical contact.

*Device B:* SEM imaging of intact switches did not show any obvious signs of damage, but the switch geometry makes contact pads not viewable without destroying the switch.

Detailed materials analysis of both devices was beyond the scope of this test.

### 6.2 Insertion Loss and Isolation

*Note:* Accuracy of the plotted data is assumed to be less than 0.05 dBm (flexing of cables can create several hundredths of a dB variation). Small steps evident in insertion loss plots correspond to 0.01dB resolution of the data. There are, however, a number of discrete steps of substantially larger variation that warrant further investigation.

*Device A:* Insertion loss and isolation values for the TxRx device are summarized in Table 2. These values reflect the performance of the TxRx entire packaged device and are not to be read as parameters of the individual MEMS switches.

| | Isolation (30 dBm) | Insertion Loss (30 dBm) | Isolation (32 dBm) | Insertion Loss (32 dBm) |
|---|---|---|---|---|
| Tx | 39.4-40.1 dB | 0.5 – 0.7 dB | 37.4 – 37.6 dB | 0.5 – 0.6 dB |
| Rx | 38.7-39.0 dB | 0.1 - 0.4 dB | 37.3 – 37.4 dB | 0.3 – 0.4 dB |

**Table 2. Device A isolation and insertion loss values.**

<u>30 dBm Results:</u>

Insertion loss (30 dBm RF input power) of the Rx switch in Figure 11 shows many abrupt steps that are well within measurement accuracy. For the first ~1.2 million cycles, the insertion loss varies greater than 0.2 dB. After this point, the average insertion loss permanently drops by 0.05 dB. In between these steps there are relatively consistent periods wherein variations are less than measurement accuracy. These variations appear to correspond to features in the Tx switch isolation plot shown below (Figure 12).

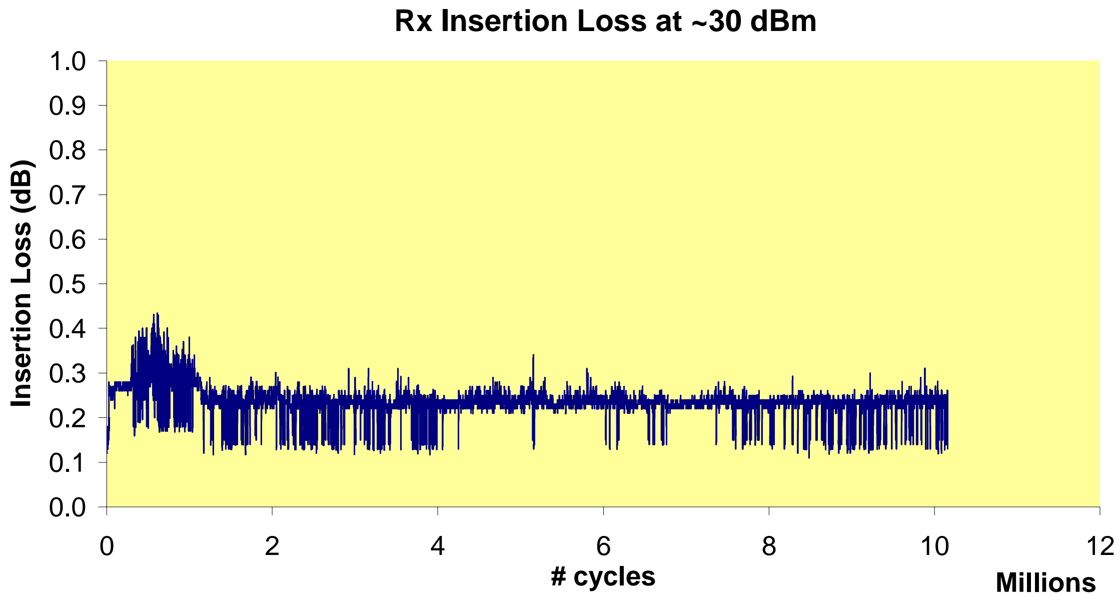


**Figure 11. Device A Rx insertion loss at 30 dBm input RF power.**

Tx isolation shown in Figure 12 (30 dBm input RF) also shows many steps of ~0.3-0.4 dB. Some of these correspond in time to features in the Rx insertion loss (Figure 11). The average value shifts from 39.75 dB to 40.1 dB between 2-4 million cycles. Note that the Tx path has two RF MEMS switches in parallel. Variations shown in the plot above are substantially larger than in the Rx isolation (single switch) shown below.

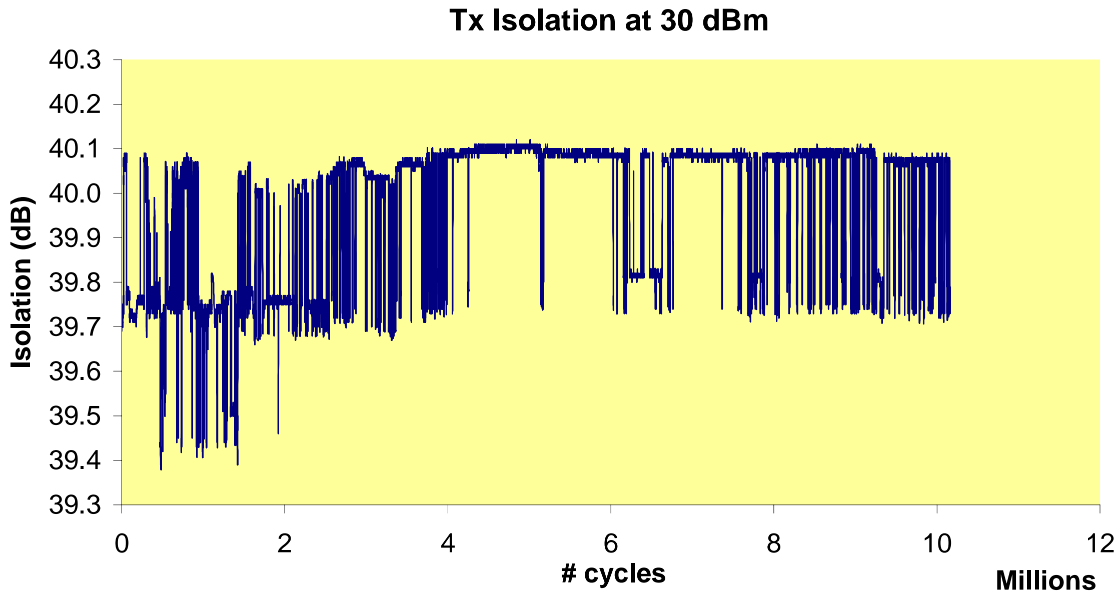


**Figure 12. Device A Tx isolation at 30 dBm input RF power.**

Rx isolation progressively decreases from 39.0 to 38.9 over the first 0.5 million cycles followed by several large 0.2-0.3 dB dips. It then decreases another 0.1 dB between 1.2 million

to 2 million cycles. Thereon it remains constant to the end of the test. The 0.2 dB variation seen in the Tx isolation are not evident in the data for this switch.

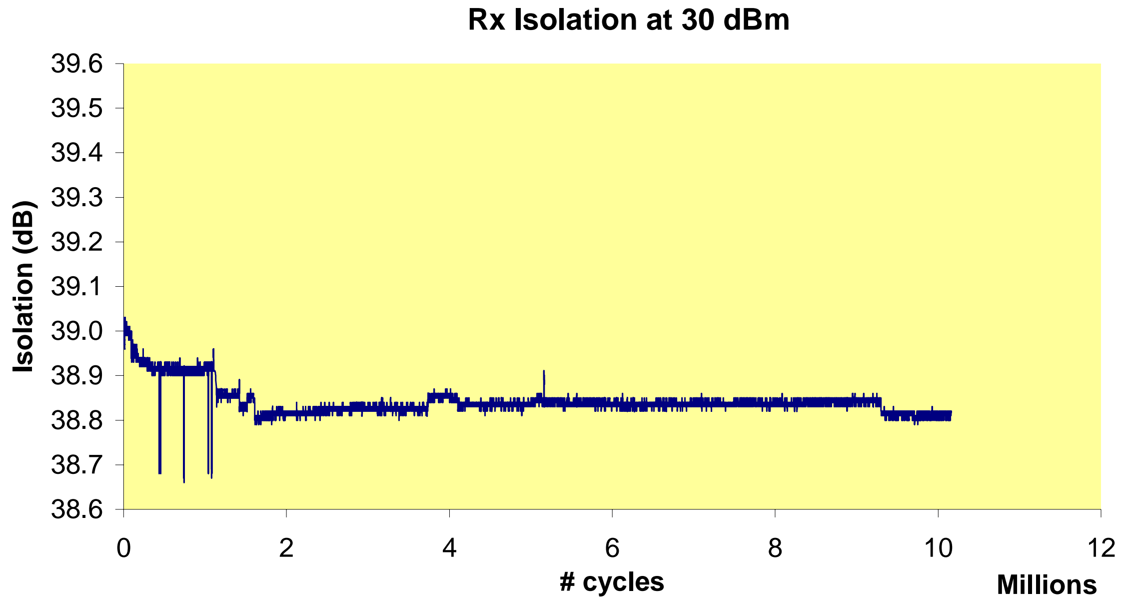


**Figure 13. Device A Rx isolation at 30 dBm input RF power.**

Like the Rx isolation results above, Tx insertion loss data (Figure 14) is much quieter than the Rx insertion loss data. Therefore, Configuration 1 appears to be more consistent over time.

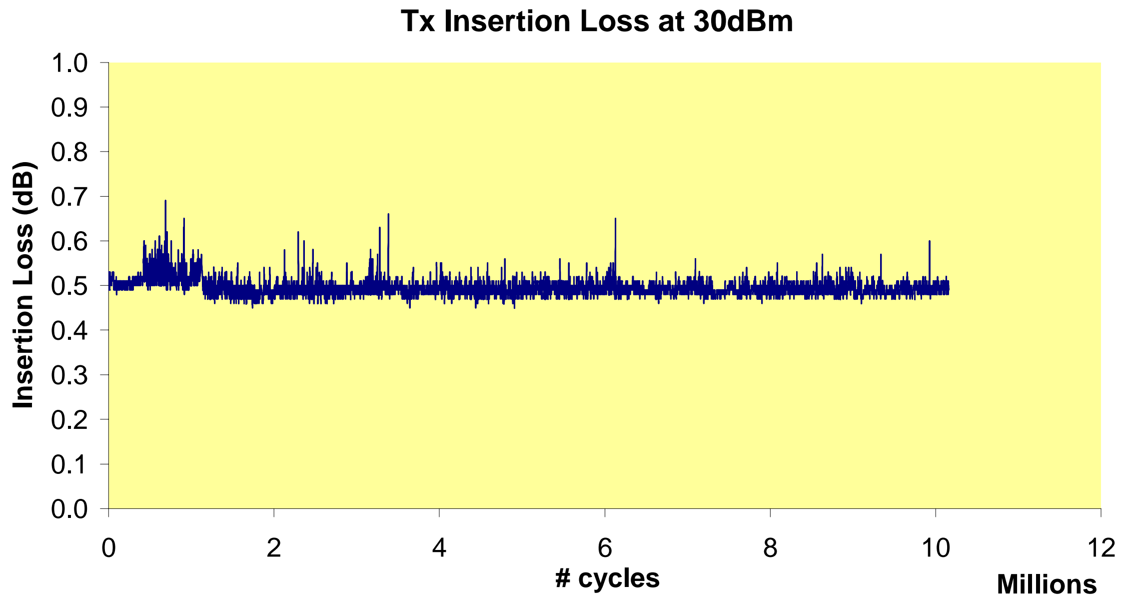


**Figure 14. Device A Tx insertion loss for 30 dBm input RF power.**

*32 dBm results:* As shown in the plots below (see Figure 15 - Figure 18), Tx path fails open after an additional 8 million cycles at 32 dBm. This indicated that both Tx switches have failed open. Average Rx insertion loss increases ~0.11 dB over the 30 dBm level of 0.25 dB. Prior to failure, Tx and Rx insertion loss both appear more consistent than at 30dBm with variations on the order of measurement accuracy. Tx isolation shows a slight but steady decrease of 0.1 dB until fail. The Rx isolation appears to abruptly decrease at the time of the open Tx path fail. However, this could be an artifact caused by the sudden increase in VSWR (Voltage Standing Wave Ratio) on the input when both paths (Tx and Rx) are simultaneously open.

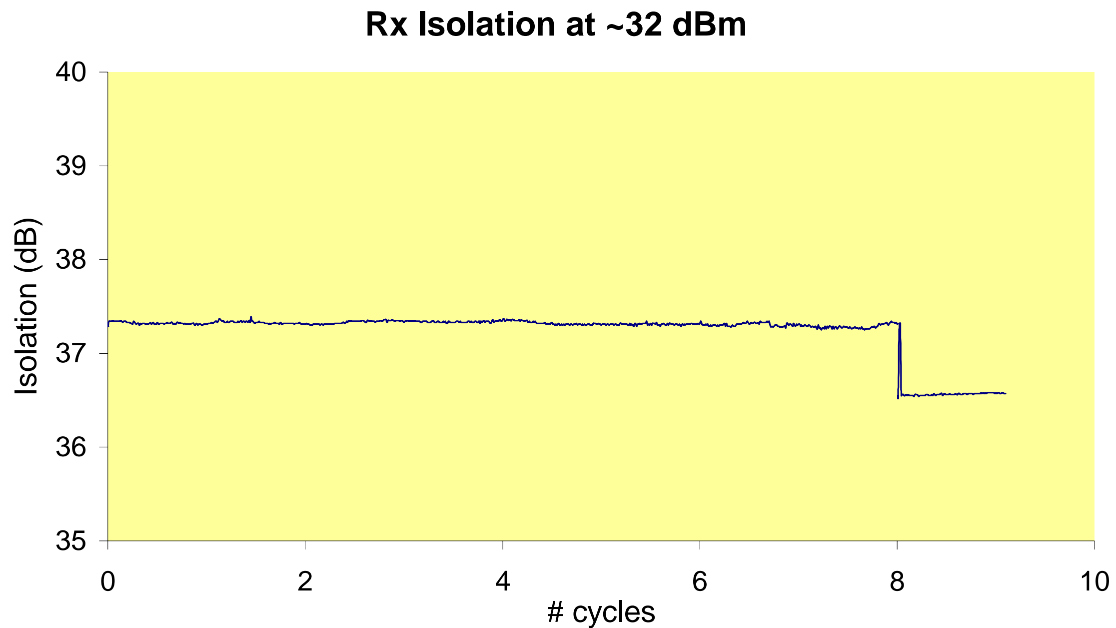


**Figure 15. Device A Rx isolation for 32 dBm input RF power.**

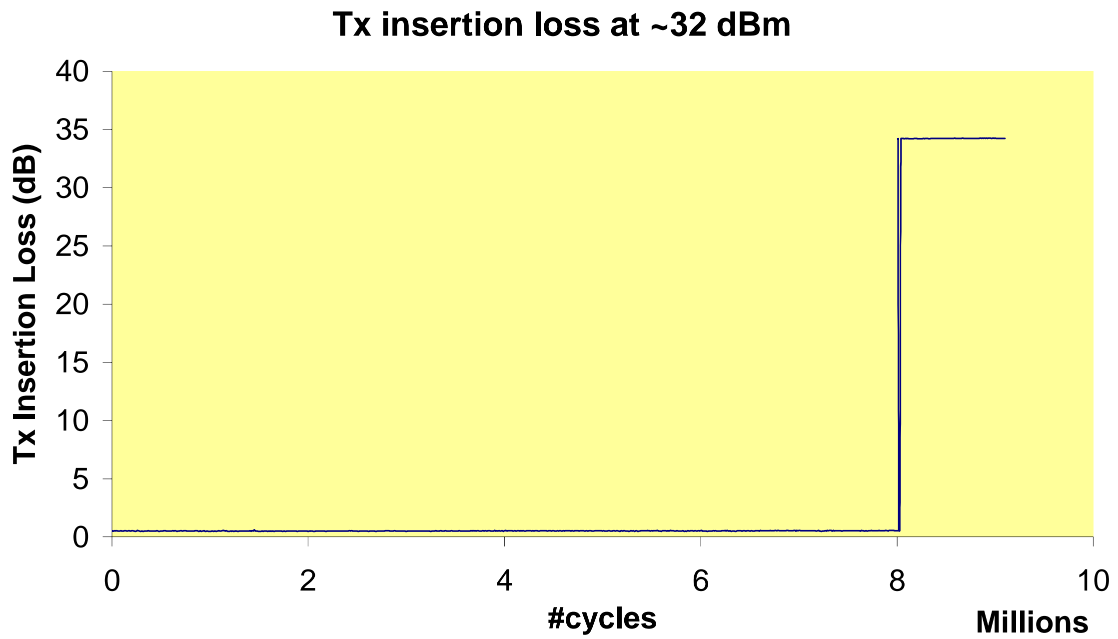


**Figure 16. Device A Tx insertion loss at 32 dBm input RF power.**

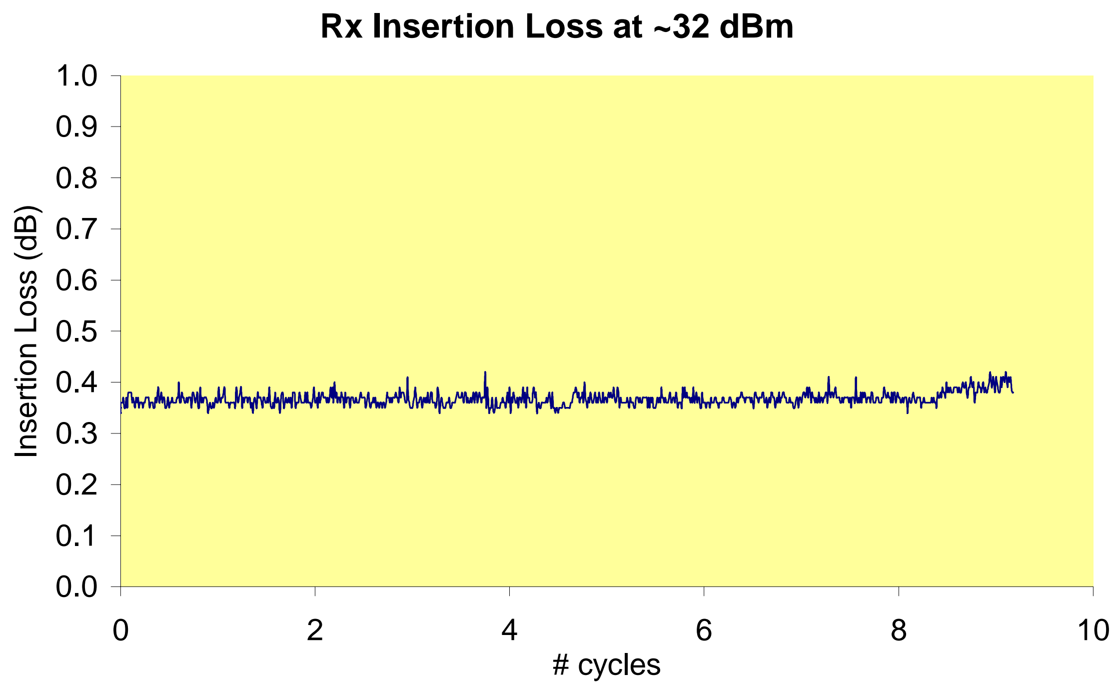


**Figure 17. Device A Rx insertion loss at 32 dBm input RF power.**

**Figure 18. Device A Tx isolation at 32 dBm input RF power.**

## 7.0 *CONCLUSIONS*

The RSC RF MEMS TxRx device performed as desired for >18 million cycles at cold-switched 1-1.5 W RF input power at 915 MHz. However, the devices proved to be fragile to hot switching and readily failed if toggled while RF power was applied. The manufacturer specified that hot switching should not be performed for this reason and considerable effort was invested in the test setup and control program to ensure adequate dwell time between power down and toggle. However, in practice, any intermittent connection between the actuation voltage source and the switch control pins (or anywhere else in the control logic chain) could result in spurious switching events while RF power is applied. With solid state technology spurious switching events would be an annoyance, but with this MEMS switch they result in permanent catastrophic failure of the part. Extreme care would be required during development, integration and test of any circuit using this part to ensure survival. However, these results are specific to this particular switch and any design changes could have a significant effect on the ruggedness.

Radiation effects tests were performed under the FY03 NEPP MEMS Radiation Effects task at JPL on this design and a more recent modification and results are published elsewhere[5].

## 8.0 *RECOMMENDATIONS FOR FURTHER TESTING*

Because failure modes in MEMS switches are highly design-dependent, limited conclusions can be drawn from reliability and performance characterization tests performed on evolving designs. Once stable switch designs become available in quantity, further testing will be required to more fully evaluate reliability and lifetime for space flight applications. Recommended tests on further designs for space flight qualification should include all the standard parameters specified by switch manufacturers, including isolation and insertion loss and intercept point over temperature and RF power. Additional parameters relevant to space flight

that a commercial manufacturer may not specify would include vibration, mechanical shock, and radiation testing.

Performing tests on a large number of devices would provide meaningful statistical conclusions and also compensate for unexpected losses due to handling and test fixture problems, as presented above. Also, in future tests, single switches instead of parallel combinations, as in the TxRx device case, would allow more direct observation of switch performance and would clarify the results.

Ruggedness tests performed under various VSWR environments should also be a priority since TxRx switches in practice are connected to antennas with poor return loss characteristics.

In addition, future measurements should be performed using a vector network analyzer to directly measure the insertion loss and isolation, rather than inferring these values from input and output power measurements that can be affected by VSWR.

## 9.0 ACKNOWLEDGEMENTS

This work was carried out at the Jet Propulsion Laboratory, California Institute of Technology, under contract with the National Aeronautics and Space Administration, Code AE, under the NASA Electronics Parts and Packaging Program (NEPP).

The authors would like to thank Thomas George, Ron Ruiz, and Manuel Gallegos of the Jet Propulsion Laboratory, David Hinkley and Ernest Robinson of the Aerospace Corporation, and Robert Mihailovich and Jeff Denatale of Rockwell Scientific Corporation for providing the coordination and assistance necessary to the success of the tests reported herein.

---

[1] "MEMS in Consumer Electronics Not Child's Play Anymore," In-Stat/MDR (www.instat.com) report, November 13, 2002.

[2] Robert F. Leheny "An Overview of Microsystems Technology Office Programs", presented at DARPA Tech 2002, July 30, 2002, http://www.darpa.mil/mto/background/index.html

[3] G. Rebeiz and J. Muldavin, "RF MEMS Switches and Switch Circuits," IEEE Microwave Magazine, pp. 59-71, Dec. 2001.

[4] R.E. Mihailovich et. al., "MEM Relay for Reconfigurable RF Circuits," Microwave and Wireless Components Letters, vol. 11, no. 2, p. 53, 2001.

[5] S. McClure *et. al.* IEEE Transactions on Nuclear Science, Vol. 49, to be published.

# **APPENDIX:**

LabVIEW code

## Connector Pane

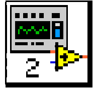

**memstestjw9.vi**

## Front Panel

stop

Total Cycles
1000

subloop#
1000

Dwell Time
100

Cycle#
999

file path
D:\National

switch C

Switch D

Power 1, dBm
9.54

Power 2 string
-2.88975699E+

Power 2, dBm
-28.90

Power 3 string
+8.97093005E+

Power 3, dBm
8.97

Power Meters 1,2,3 - State 1

PM1
PM2
PM3

Amplitude
10.0
0.0
-10.0
-20.0
-30.0
-40.0
-50.0
-60.0
0
Time

Power Meters 1,2,3 - State 2

PM1
PM2
PM3

Amplitude
10.0
0.0
-10.0
-20.0
-30.0
-40.0
-50.0
-60.0
0
100
Time

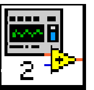

memstestjw9.vi

## Block Diagram

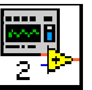

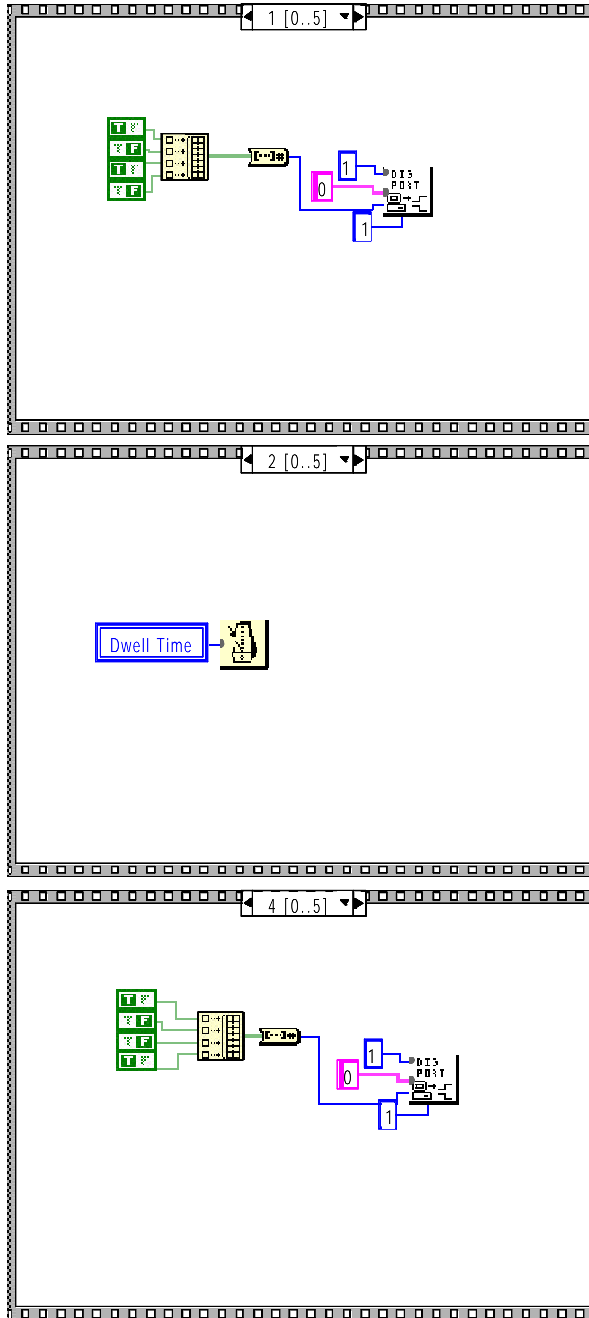
1 [0..5]
1
0
1
2 [0..5]
Dwell Time
4 [0..5]
1
0
1

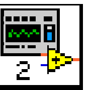

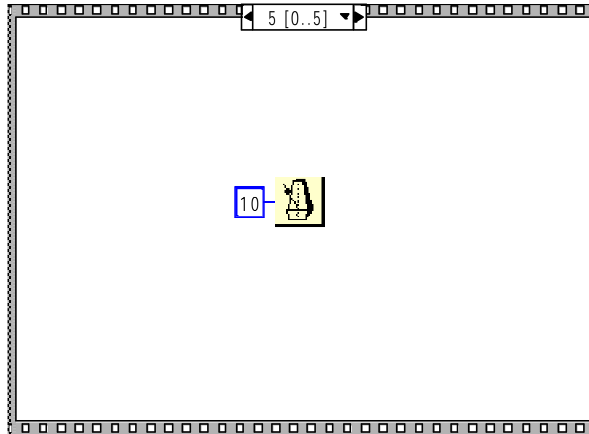
5 [0..5]
10

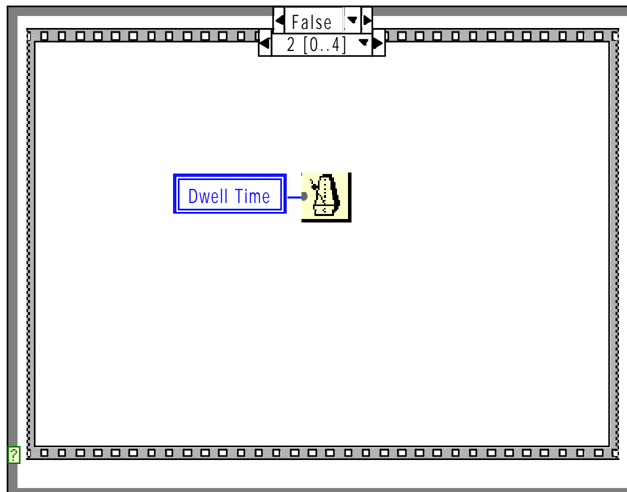
False
2 [0..4]
Dwell Time

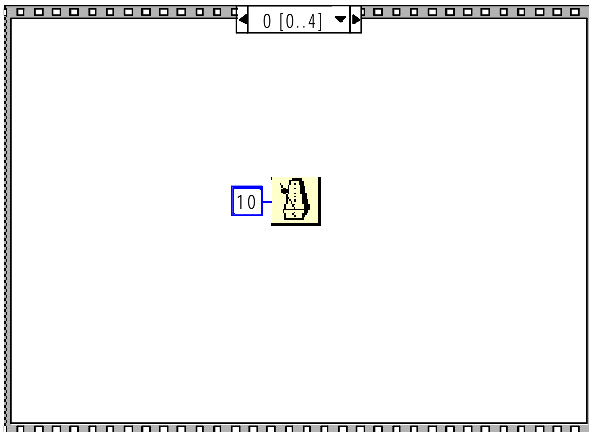
0 [0..4]
10

memstestjw9.vi



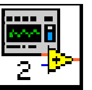

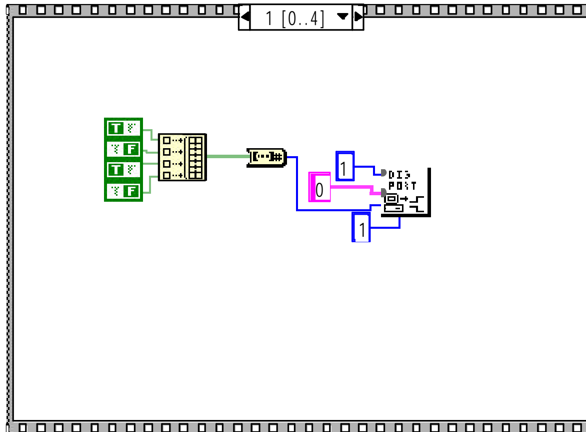


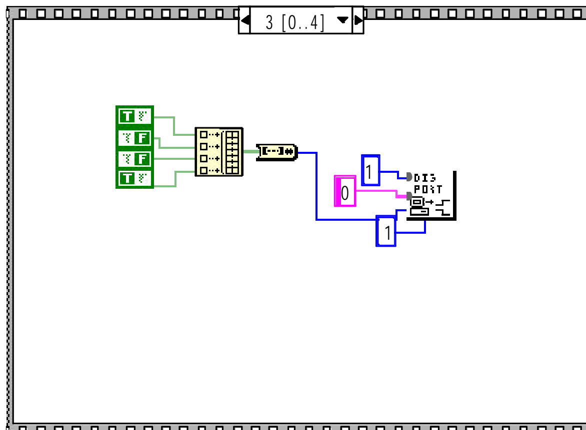


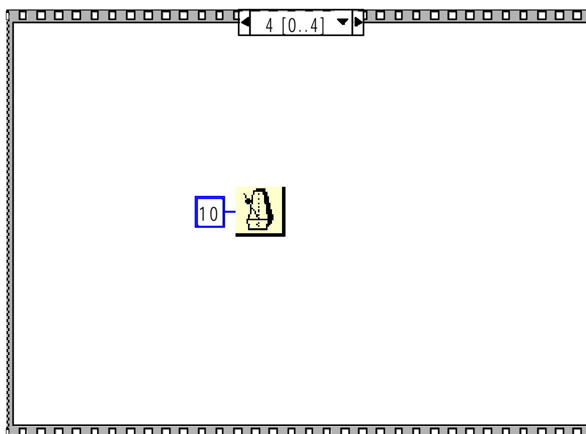

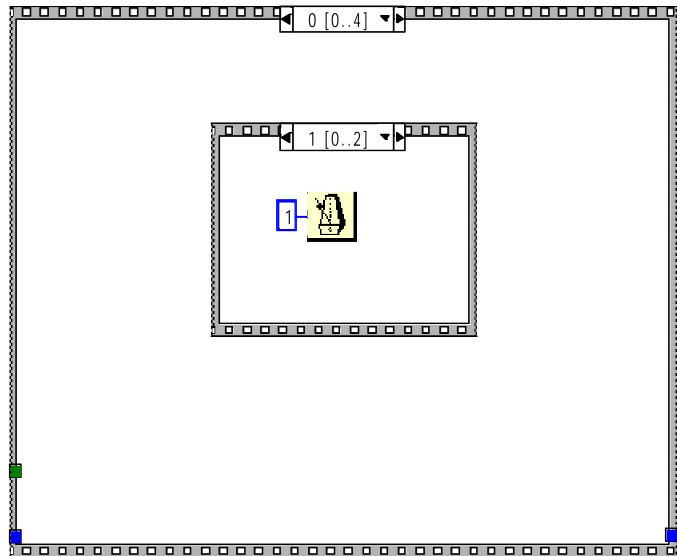
0 [0..4]
1 [0..2]
1

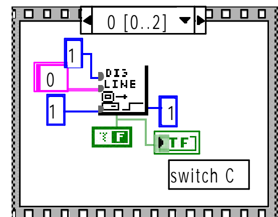
0 [0..2]
1
0
1
1
switch C

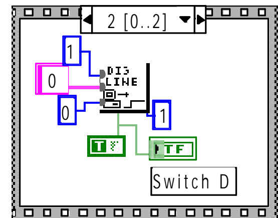
2 [0..2]
1
0
0
1
Switch D

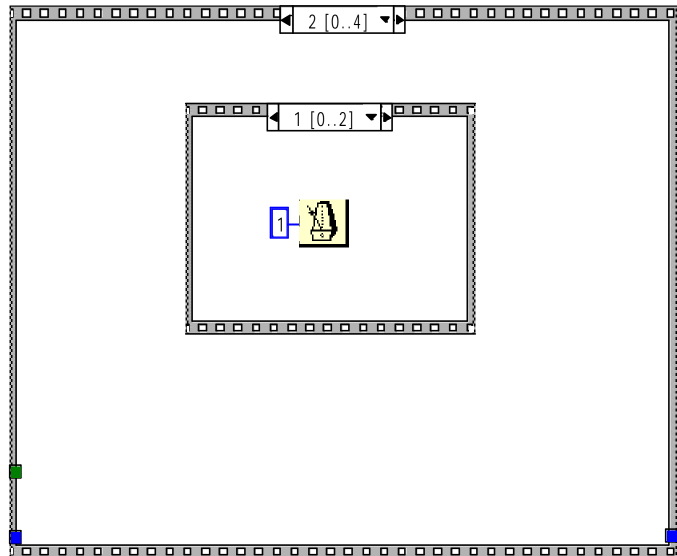
2 [0..4]
1 [0..2]
1

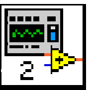

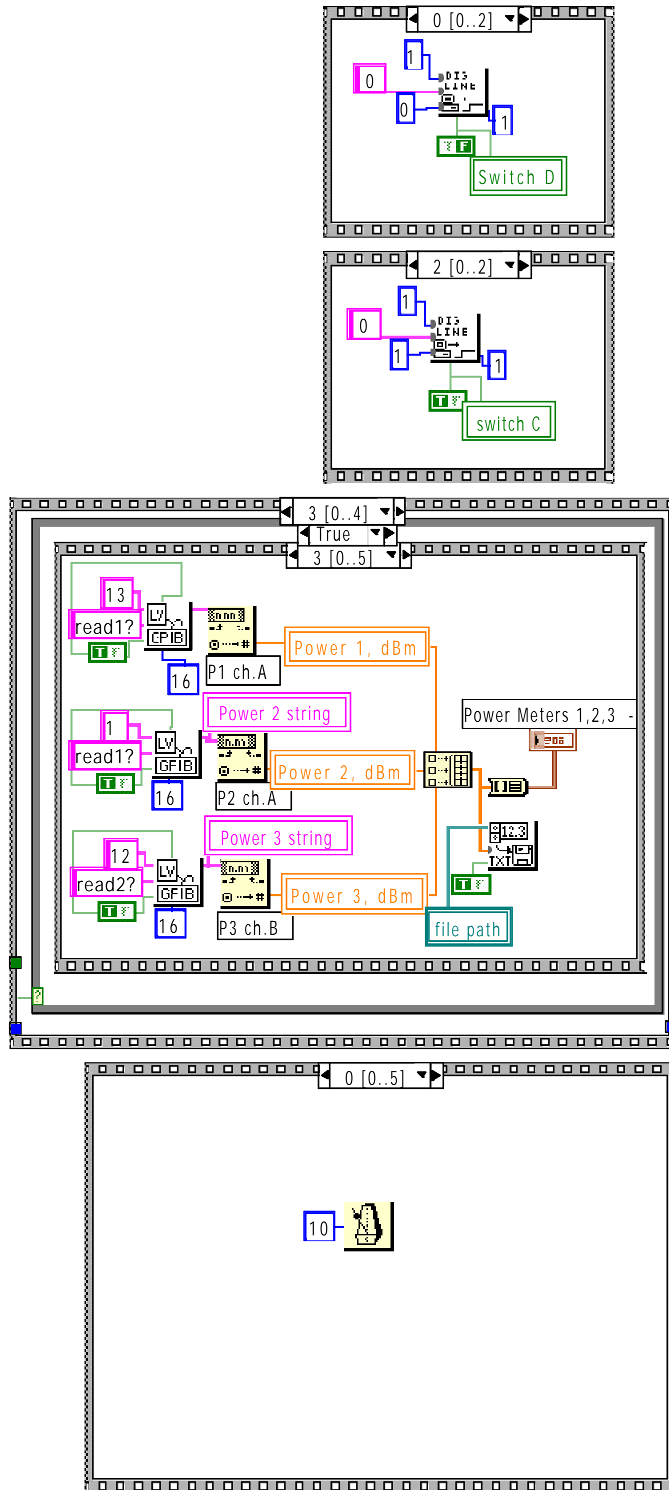

0 [0..2]
1
0
0
1
Switch D
2 [0..2]
0
1
1
1
switch C
3 [0..4]
True
3 [0..5]
13
read1?
16
P1 ch.A
Power 1, dBm
Power 2 string
Power Meters 1,2,3
1
read1?
16
P2 ch.A
Power 2, dBm
Power 3 string
12
read2?
16
P3 ch.B
Power 3, dBm
file path
0 [0..5]
10

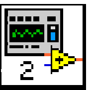

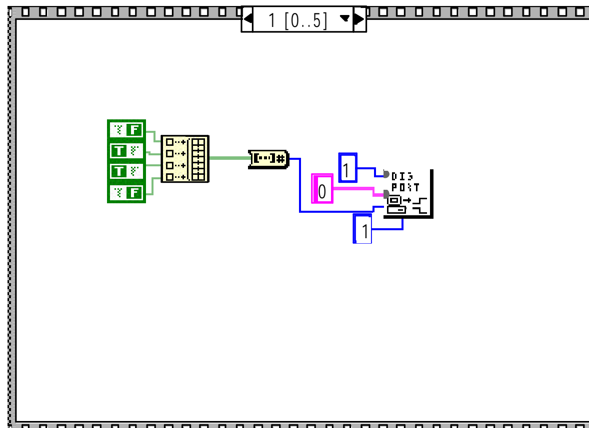
1 [0..5]
1
0
1

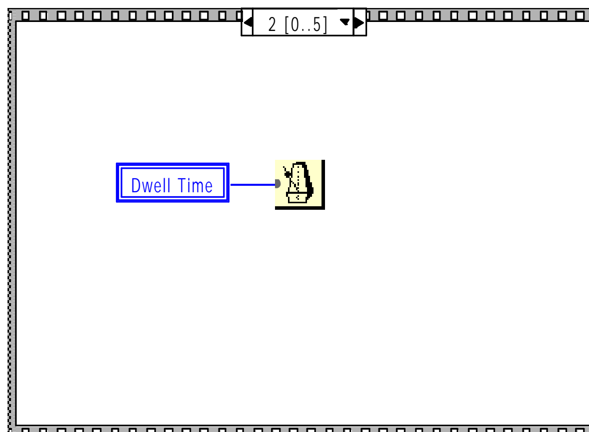
2 [0..5]
Dwell Time

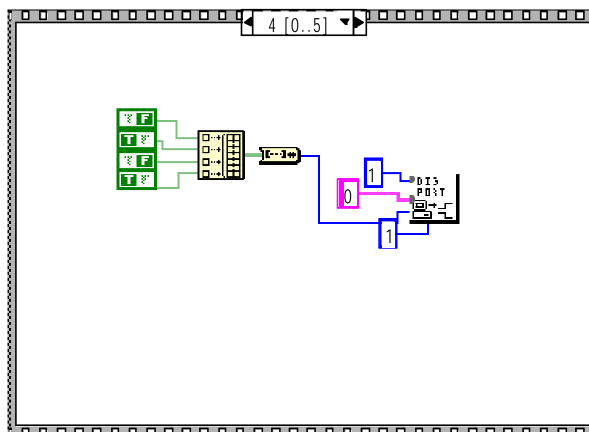
4 [0..5]
1
0
1

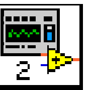

memstestjw9.vi

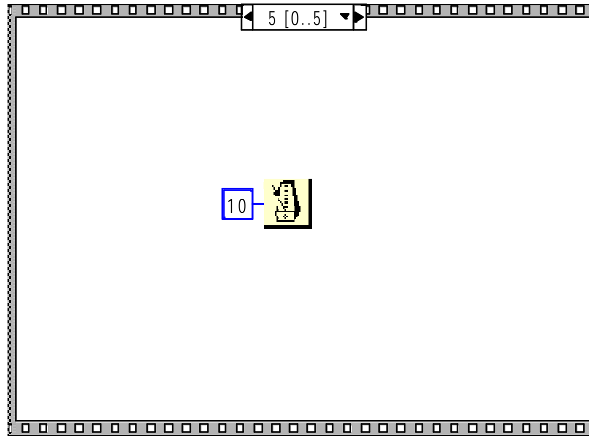


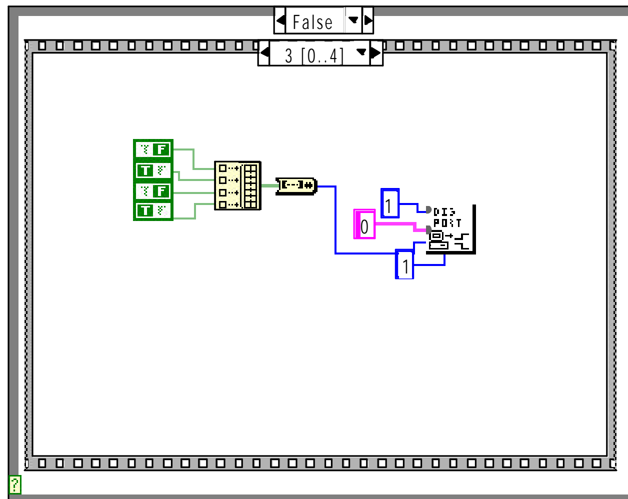


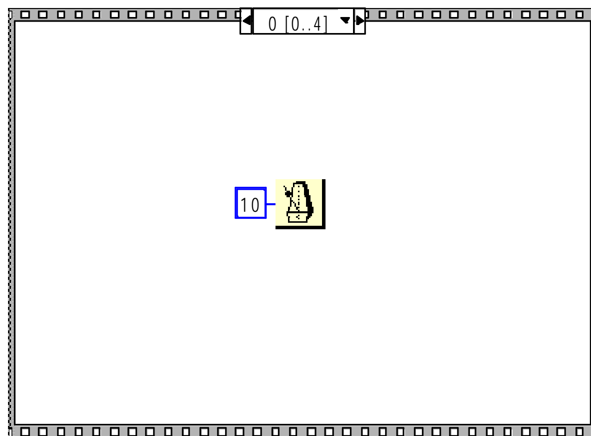

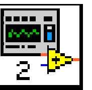

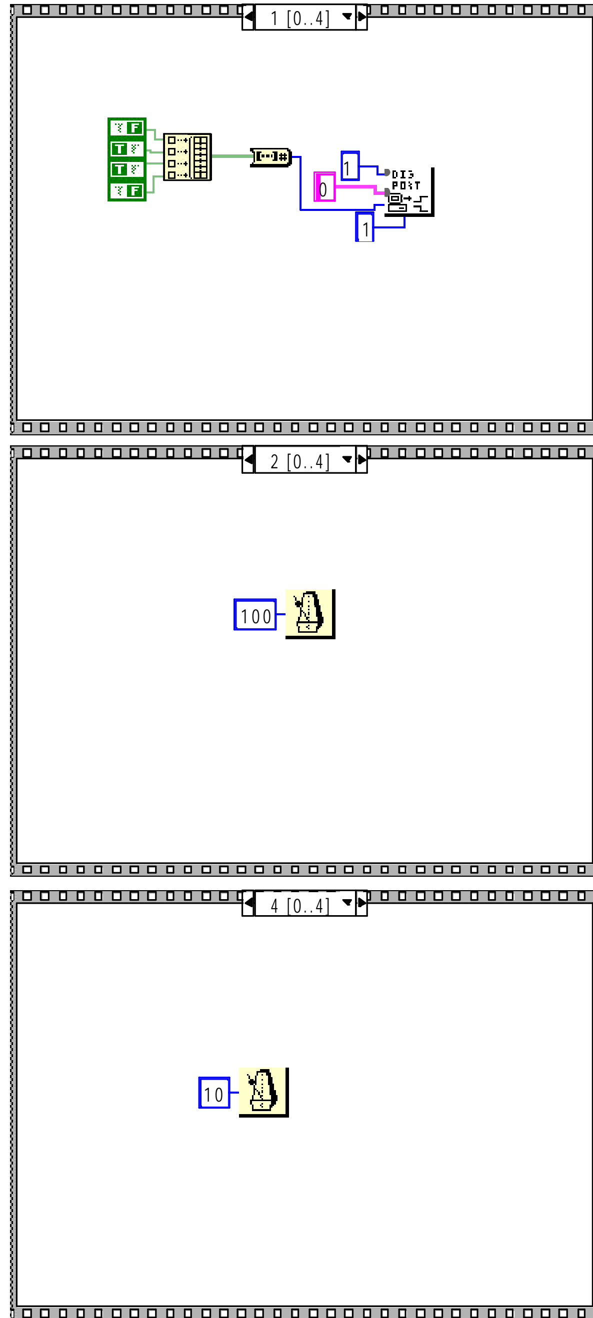
1 [0..4]
1
0
DIG PORT
1
2 [0..4]
100
4 [0..4]
10

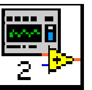

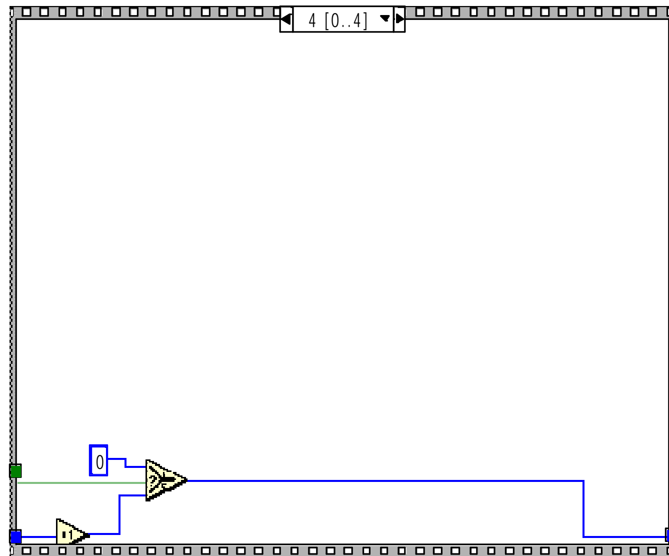
4 [0..4]
0

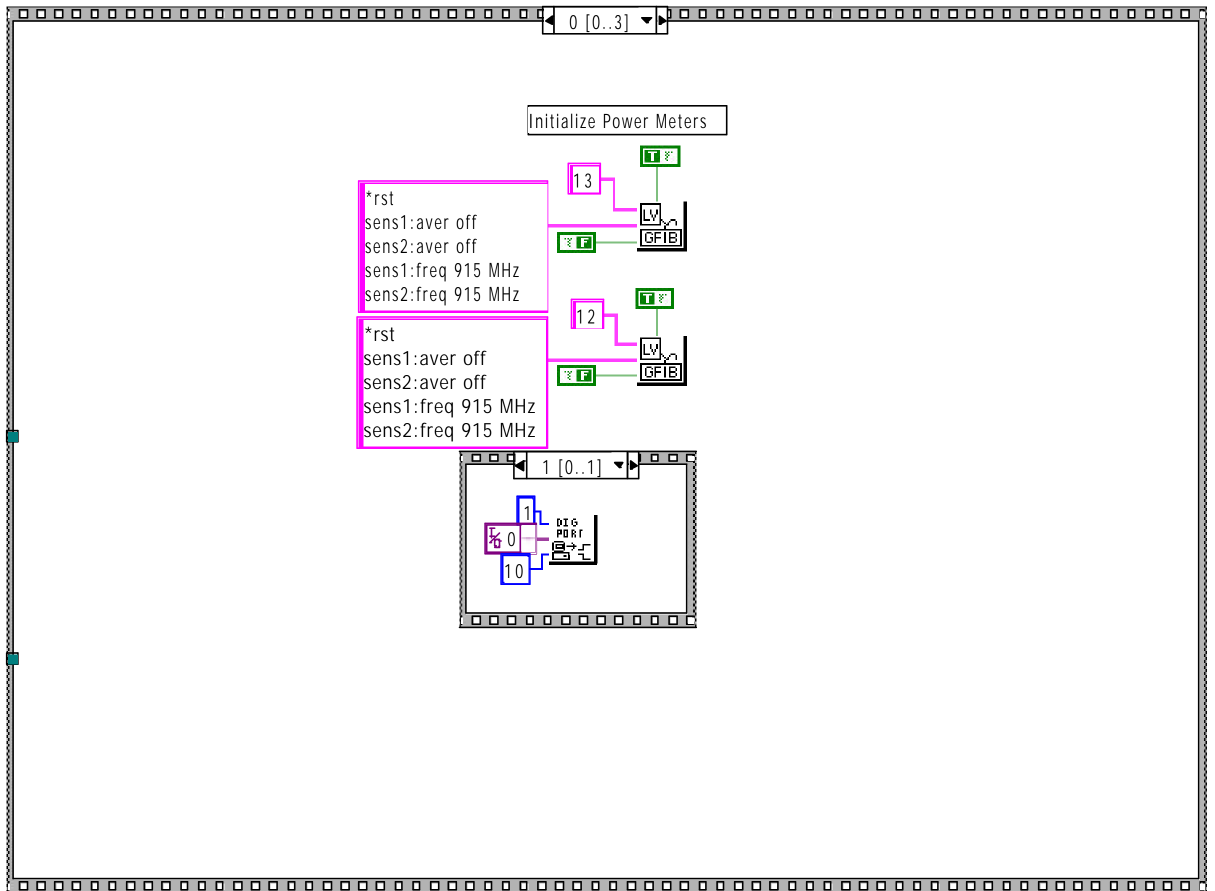
0 [0..3]
Initialize Power Meters
13
*rst
sens1:aver off
sens2:aver off
sens1:freq 915 MHz
sens2:freq 915 MHz
12
*rst
sens1:aver off
sens2:aver off
sens1:freq 915 MHz
sens2:freq 915 MHz
1 [0..1]
1
0
10

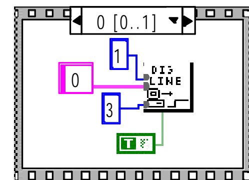
0 [0..1]
1
0
3

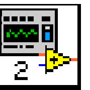

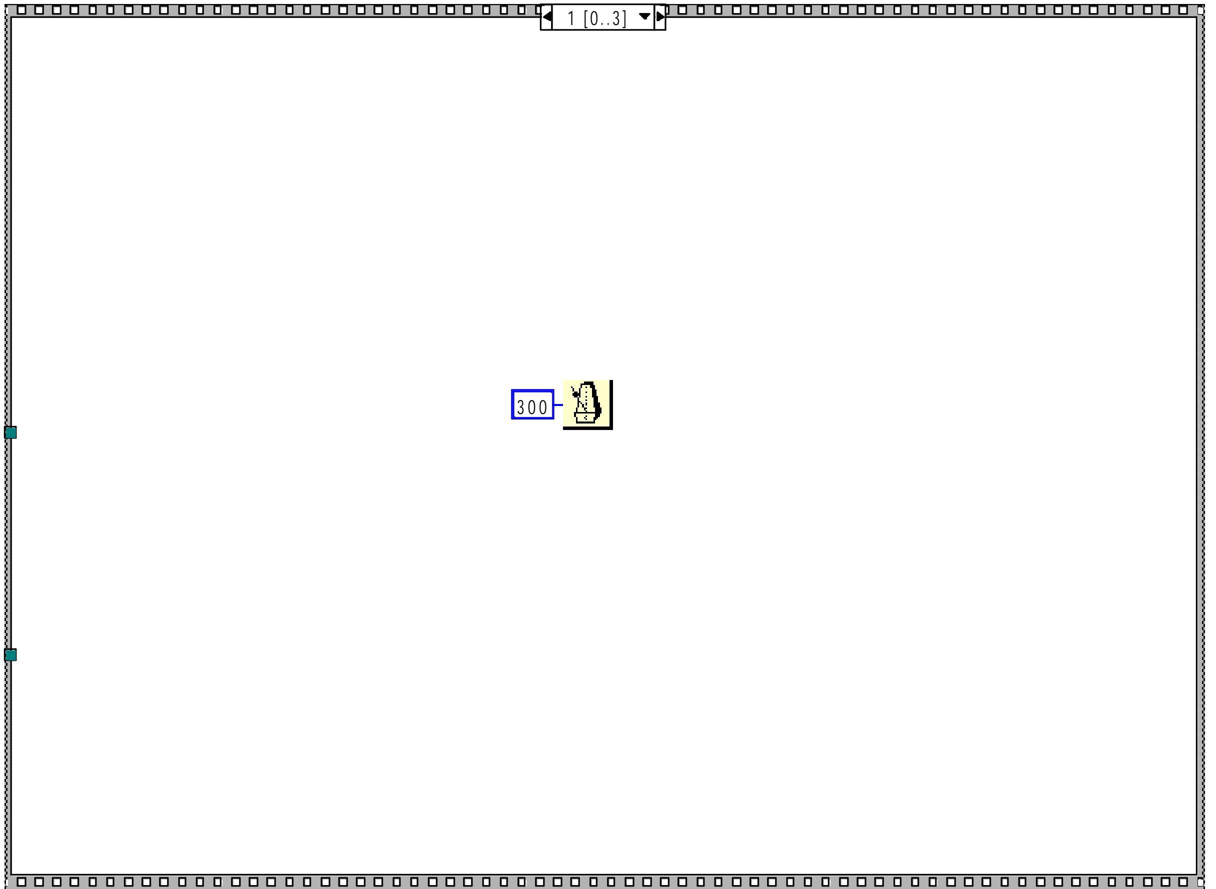

1 [0..3]
300

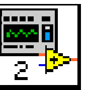

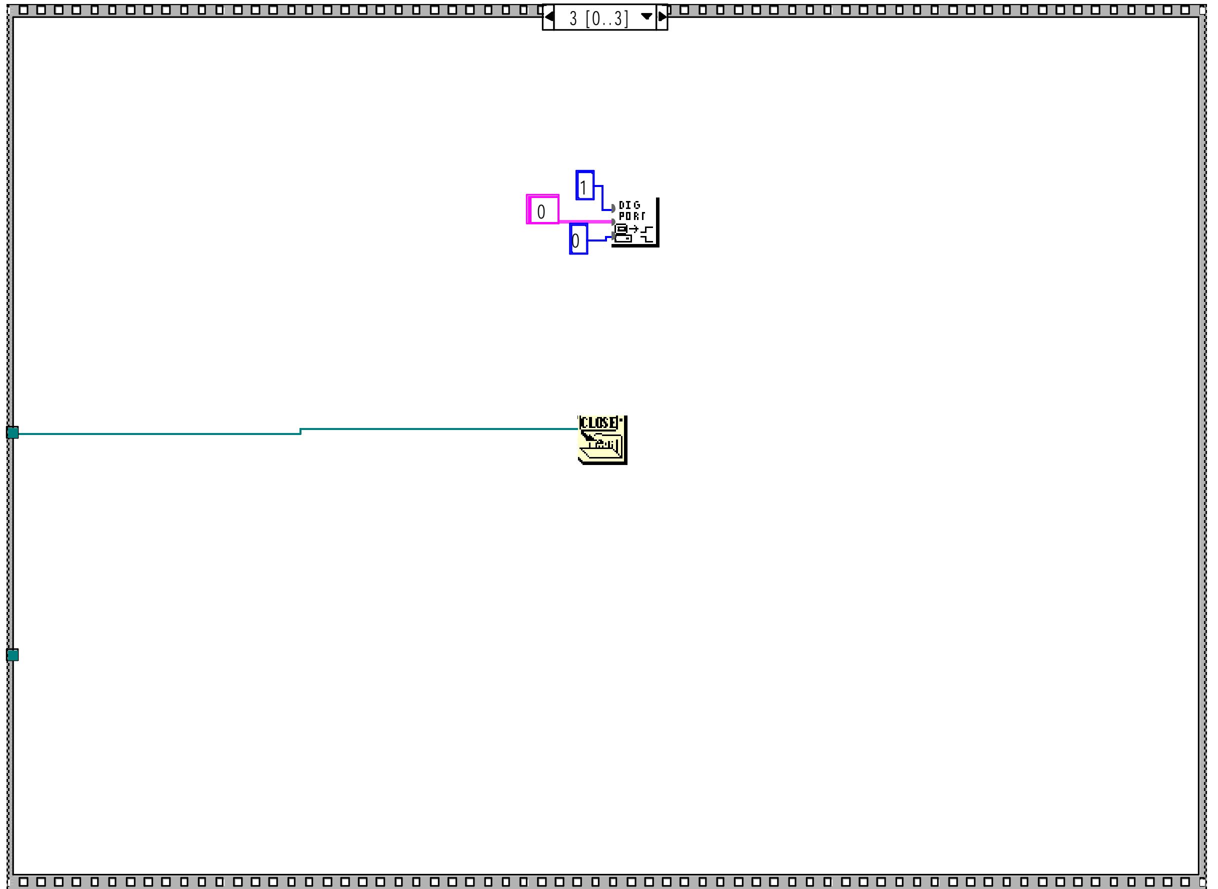
3 [0..3]
1
0
DIG PORT
0
CLOSE